Effects of ion-neutral collisions on Alfvén waves: The presence of forbidden zone and heavy damping zone

C. J. Weng, L. C. Lee, C. L. Kuo, and C. B. Wang

Citation: Physics of Plasmas (1994-present) **20**, 032902 (2013); doi: 10.1063/1.4796043
View online: http://dx.doi.org/10.1063/1.4796043
View Table of Contents: http://scitation.aip.org/content/aip/journal/pop/20/3?ver=pdfcov
Published by the AIP Publishing

Effects of ion-neutral collisions on Alfvén waves: The presence of forbidden zone and heavy damping zone

C. J. Weng,[1,2] L. C. Lee,[2,3,a)] C. L. Kuo,[2] and C. B. Wang[4]
[1]*Department of Physics, National Cheng Kung University, Tainan 701, Taiwan*
[2]*Institute of Space Science, National Central University, Jhongli 320, Taiwan*
[3]*Institute of Earth Science, Academia Sinica, Nankang 115, Taiwan*
[4]*CAS Key Laboratory of Geospace Environment, School of Earth and Space Sciences, University of Science and Technology of China, Hefei, China*

(Received 30 August 2012; accepted 4 March 2013; published online 21 March 2013)

Alfvén waves are low-frequency transverse waves propagating in a magnetized plasma. We define the Alfvén frequency ω_0 as $\omega_0 = kV_A\cos\theta$, where k is the wave number, V_A is the Alfvén speed, and θ is the angle between the wave vector and the ambient magnetic field. There are partially ionized plasmas in laboratory, space, and astrophysical plasma systems, such as in the solar chromosphere, interstellar clouds, and the earth ionosphere. The presence of neutral particles may modify the wave frequency and cause damping of Alfvén waves. The effects on Alfvén waves depend on two parameters: (1) $\alpha = n_n/n_i$, the ratio of neutral density (n_n), and ion density (n_i); (2) $\beta = \nu_{ni}/\omega_0$, the ratio of neutral collisional frequency by ions ν_{ni} to the Alfvén frequency ω_0. Most of the previous studies examined only the limiting case with a relatively large neutral collisional frequency or $\beta \gg 1$. In the present paper, the dispersion relation for Alfvén waves is solved for all values of α and β. Approximate solutions in the limit $\beta \gg 1$ as well as $\beta \ll 1$ are obtained. It is found for the first time that there is a "forbidden zone (FZ)" in the $\alpha - \beta$ parameter space, where the real frequency of Alfvén waves becomes zero. We also solve the wavenumber k from the dispersion equation for a fixed frequency and find the existence of a "heavy damping zone (HDZ)." We then examine the presence of FZ and HDZ for Alfvén waves in the ionosphere and in the solar chromosphere. © *2013 American Institute of Physics*. [http://dx.doi.org/10.1063/1.4796043]

I. INTRODUCTION

Alfvén waves are low-frequency transverse waves in a magnetized plasma and are widely studied in laboratory plasmas, space plasmas, and astrophysical plasmas.[1–12] It is generally believed that Alfvén waves play an important role in the heating of solon chromosphere, solar corona, and magnetic fusion plasma,[2,6–15] in the transportation of cosmic rays in the interstellar medium,[3,16] and in the coupling interaction between ionosphere, magnetosphere, and solar wind.[7,11,17]

There are partially ionized plasmas in most space and astrophysical plasma systems, such as in the solar chromosphere, protostellar disks, interstellar and circumstellar clouds, the earth ionosphere, and nuclear fusion devices. Neutral atoms may affect the plasma dynamics and hence Alfvén waves through collisions with charged particles. Alfvén indicated that the collisions between ionized fluid and neutral gas with the high ionization rate are important in the planetary system.[18] Piddington,[19,20] Lehnert,[21] and Osterbrock[22] pointed out that the effect of collisions may lead to absorption of plasma waves in the chromosphere, photosphere, and interstellar clouds. Hartmann and MacGregor studied damping of Alfvén waves in stellar winds.[23] Zweibel examined the effect of ion-neutral collisions on magnetic reconnection in solar prominences and molecular clouds.[24] Huba examined the universal interchange instability in partially ionized gases.[25] Haerendel,[26] De Pontieu and Haerendel,[27] De Pontieu *et al.*,[28] James and Erdélyi,[29] James *et al.*,[30] and Erdélyi and James[31] suggested that the energy and momentum transfer from damping Alfvén waves through ion-neutral collisions in the partially ionized chromospheric plasma may provide a formation mechanism for spicules.

A number of publications have discussed the damping of Alfvén waves by ion-neutral collisions. The general dispersion equations for magnetohydrodynamic waves in the partially ionized medium have been derived in many studies.[2,3,26,28,32–39] It is well established that the dispersion relation of Alfvén waves is strongly influenced by the ion-neutral collisions in partially ionized plasmas.

There are two key parameters that determine the strength of coupling between neutrals and charged particles and the effects on the dispersion relation of Alfvén waves. These two parameters are (1) $\alpha = n_n/n_i$, the ratio of neutral density (n_n), and ion density (n_i); (2) $\beta = \nu_{ni}/\omega_0$, the ratio of neutral collisional frequency by ions ν_{ni} to the Alfvén frequency ω_0, where $\omega_0 = kV_A\cos\theta$, k is the wave number, V_A is the Alfvén speed in the absence of neutral particles, and θ is the angle between the wave propagating direction and the ambient magnetic field. Most of previous studies in the literature examined only the limiting cases with a relatively large neutral collisional frequency or $\beta \gg 1$.[2,3,26,28,36–40] The dispersion relation of Alfvén waves in the full $\alpha - \beta$ parameter space has not been systematically studied.

In this paper, we investigate the effect of ion-neutral collisions on the damping of Alfvén waves in a homogeneous

a)Author to whom correspondence should be addressed. Electronic mail: louclee@earth.sinica.edu.tw.

plasma. In Sec. II, the dispersion equation and eigen-modes of Alfvén waves in a partially ionized plasma are derived. In Sec. III, the dispersion relation is solved for all values of α and β. It is found for the first time that there is a "forbidden zone (FZ)" in the $\alpha-\beta$ parameter space, where the real frequency of Alfvén waves becomes zero. We also solve the wavenumber k from the dispersion equation for a given frequency and find the existence of a "heavy damping zone (HDZ)." In Sec. IV, we also try to examine the presence of FZ and HDZ for Alfvén waves in the ionosphere and in the solar chromosphere. Finally, the main results are summarized in Sec. V.

II. FORMULATIONS

A. Basic equations for fluid with ions and neutrals

We calculate the effect of collisions between ions and neutrals on the propagation of transverse Alfvén waves in a homogeneous magnetized plasma. The plasma fluid consists of two components: ionized particles (ions and electrons) and neutral particles. The continuity equations, momentum equations, and energy equations for the two components can be written as

$$\frac{\partial \rho_i}{\partial t}+\nabla\cdot(\rho_i \boldsymbol{v}_i)=0, \tag{1}$$

$$\frac{\partial \rho_n}{\partial t}+\nabla\cdot(\rho_n \boldsymbol{v}_n)=0, \tag{2}$$

$$\rho_i\left[\frac{\partial \boldsymbol{v}_i}{\partial t}+(\nabla\cdot\boldsymbol{v}_i)\boldsymbol{v}_i\right]=-\nabla p_i+\frac{1}{\mu_0}(\nabla\times\mathbf{B})\times\mathbf{B} -\rho_i\nu_{in}(\boldsymbol{v}_i-\boldsymbol{v}_n), \tag{3}$$

$$\rho_n\left[\frac{\partial \boldsymbol{v}_n}{\partial t}+(\nabla\cdot\boldsymbol{v}_n)\boldsymbol{v}_n\right]=-\nabla p_n-\rho_n\nu_{ni}(\boldsymbol{v}_n-\boldsymbol{v}_i). \tag{4}$$

The Faraday's equation and the generalized Ohm's law can be written as

$$\frac{\delta B}{\delta t}=-\nabla\times\mathbf{E}, \tag{5}$$

$$n_e e(\mathbf{E}+\mathbf{v}\times\mathbf{B})-\boldsymbol{J}\times B-(m_e/e)(\nu_{ei}+\nu_{en})\boldsymbol{J}=0. \tag{6}$$

Here $\mathbf{B}$ is the magnetic field, $\boldsymbol{J}=\nabla\times\mathbf{B}/\mu_0$ is the current density, ρ is mass density, p is the pressure, $\boldsymbol{v}$ is the velocity, $\boldsymbol{J}$ is the current density, and $\gamma=5/3$ is the ratio of specific heats. The subscripts "i" and "n" denote the ionized component and neutrals, respectively. We have $\rho_i=m_i n_i$ and $\rho_n=m_n n_n$. The ion collisional frequency by neutral particles is denoted by ν_{in} while the neutral collisional frequency by ions is denoted by ν_{ni}. The electron collisional frequency by ions (neutrals) is denoted by $\nu_{ei}(\nu_{en})$. We assume that the electron number density (n_e) equals to the ion number density (n_i).

For conservation of total momentum, we assume $m_i=m_n$ and obtain from Eqs. (2) and (4)

$$\alpha\equiv n_n/n_i=\nu_{in}/\nu_{ni}. \tag{7}$$

In the generalized Ohm's law of Eq. (6), the term associated with $\boldsymbol{v}\times B$ is called the advective term, $\boldsymbol{J}\times B$ term is called the Hall term, and the last one is the resistive term. Let $\Omega_e(\Omega_i)$ be the electron (ion) gyrofrequency and $\nu_e=\nu_{ei}+\nu_{en}$. It can be shown[12] that

$$\begin{aligned}\text{Hall/advective}&=\omega_0/\Omega_i \quad \text{if} \quad \beta=\nu_{ni}/\omega_0\ll 1,\\ &=\alpha\omega_0/\Omega_i \quad \text{if} \quad \beta\gg 1,\\ \text{resistive/advective}&=\alpha\omega_0\nu_e/\Omega_e\Omega_i.\end{aligned}$$

Song and Vasyliunas[12] showed that the ratios (Hall/advective) and (resistive/advective) are much smaller than one in the solar chromosphere and corona for $\omega_0<10^4$ Hz. On the other hand, the Hall term may become important in the lower part of ionosphere (altitude below 200 km) for $\omega_0\geq 10^2 s^{-1}$. The Hall term may lead to the coupling of Alfvén waves and compressional magnetosonic waves in the ionosphere.[35] The Hall term may also lead to generation of kinetic Alfvén waves from compressional mirror waves.[41] We ignore Hall and resistive terms in the following discussions.

B. Dispersion equation and eigen-modes for Alfvén waves

A very convenient geometry for studying Alfvén waves is shown in Figure 1. The waves are propagating in the z direction, and the background magnetic field is in the $y-z$ plane, $\mathbf{B}_0=B_0(\sin\theta\hat{\boldsymbol{y}}+\cos\theta\hat{\boldsymbol{z}})$, where θ is the angle between propagating vector $\boldsymbol{k}$ and magnetic field $\mathbf{B}_0$.

In the initial equilibrium state, let the ion density be ρ_{i0}, neutral density ρ_{n0}, ion velocity $\boldsymbol{v}_{i0}=0$, and neutral velocity $\boldsymbol{v}_{n0}=0$. In the presence of perturbed quantities, we have $\rho_i=\rho_{i0}+\delta\rho_i$, $\rho_n=\rho_{n0}+\delta\rho_n$, $\boldsymbol{v}_i=\delta\boldsymbol{v}_i$ and $\boldsymbol{v}_n=\delta\boldsymbol{v}_n$, and $\mathbf{B}=\mathbf{B}_0+\delta\mathbf{B}$. The x-components of perturbed equations from Eqs. (3), (4), and (6) can be written as

$$\frac{\partial \delta v_{nx}}{\partial t}=-\nu_{ni}(\delta v_{nx}-\delta v_{ix}), \tag{8}$$

$$\rho_{i0}\frac{\partial \delta v_{ix}}{\partial t}=\frac{1}{\mu_0}B_0\cos\theta\frac{\partial}{\partial z}\delta B_x-\rho_{i0}\nu_{in}(\delta v_{ix}-\delta v_{nx}), \tag{9}$$

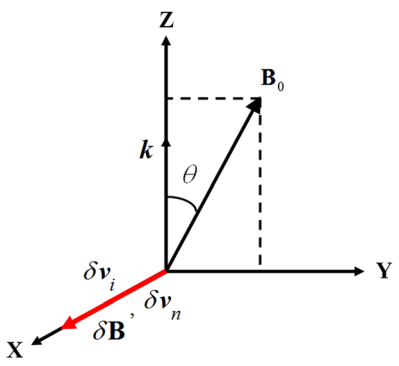

FIG. 1. Geometry for propagating Alfvén wave. The wave vector $\mathbf{k}$ is in the z direction, and the ambient magnetic field $\mathbf{B}_0$ is in the $y-z$ plane. The perturbed velocities $\delta\mathbf{v}_i$, $\delta\mathbf{v}_n$, and magnetic field $\delta\mathbf{B}$ are in the x direction.

$$\frac{\partial \delta B_x}{\partial t} = B_0 \cos\theta \frac{\partial}{\partial z} \delta v_{ix}. \tag{10}$$

We note that Eqs. (8)–(10) give the coupling equations for only δv_{ix}, δv_{nx}, and δB_x, which are decoupled from other quantities ($\delta\rho_i$, $\delta\rho_n$, δv_{iy}, δv_{iz}, δv_{ny}, δv_{nz}, δB_y, and δB_z).

Considering plane wave solutions of the form $e^{i(kz-wt)}$ with $\frac{\partial}{\partial z} = ik$ and $\frac{\partial}{\partial t} = -i\omega$, we obtain the following matrix equation from Eqs. (8)–(10):

$$\begin{bmatrix} i\omega - \nu_{in} & \nu_{in} & i\left(\frac{B_0}{\mu_0\rho_{i0}}\right)k\cos\theta \\ \nu_{ni} & i\omega - \nu_{ni} & 0 \\ B_0 k\cos\theta & 0 & \omega \end{bmatrix} \cdot \begin{bmatrix} \delta v_{ix} \\ \delta v_{nx} \\ \delta B_x \end{bmatrix} = 0. \tag{11}$$

Equation (11) yields the wave eigen-mode as

$$\begin{bmatrix} \delta B_x \\ \delta v_{ix} \\ \delta v_{nx} \end{bmatrix} = \delta B_x \begin{bmatrix} 1 \\ -\frac{\omega}{B_0 k\cos\theta} \\ \frac{\omega\nu_{ni}}{B_0 k\cos\theta(i\omega - \nu_{ni})} \end{bmatrix}. \tag{12}$$

Setting the determinant in Eq. (11) to zero, we obtain the following dispersion equation for transverse Alfvén waves:

$$\omega^3 + i(\nu_{ni} + \nu_{in})\omega^2 - V_A^2 k^2 \cos^2\theta\omega - iV_A^2 k^2 \cos^2\theta\nu_{ni} = 0, \tag{13}$$

where $V_A = (B_0/\mu_0\rho_{i0})^{1/2}$ is the Alfvén speed in the absence of neutral particles. The dispersion equation (13) has been obtained by many authors. The dispersion equations (13) and (14) can also be used for oblique propagation with Alfvén frequency $\omega_0 = kV_A\cos\theta$.

Set $\alpha \equiv \frac{\rho_n}{\rho_i} = \frac{n_n}{n_i} = \frac{\nu_{in}}{\nu_{ni}}$ and $\beta \equiv \frac{\nu_{ni}}{\omega_0}$. Here ω_0 is the Alfvén frequency in the absence of neutral particles and α is the ratio of neutral and ion density. We can write the normalized quantities as following: $\delta v_{ix}^* = \delta v_{ix}/V_A$, $\delta v_{nx}^* = \delta v_{nx}/V_A$, $\omega^* = \omega/\omega_0$, and $\delta B_x^* = \delta B_x/B_0$. In the following discussions, we drop the sign "*" associated with normalized quantities for convenience. In the normalized forms, we obtain from Eqs. (12) and (13) the simplified dispersion relation and eigen-relations of Alfvén waves as

$$\omega^3 + i(1+\alpha)\beta\omega^2 - \omega - i\beta = 0, \tag{14}$$

$$\delta v_{ix} = -\omega\delta B_x, \tag{15}$$

$$\delta v_{nx} = \frac{\omega\beta}{i\omega - \beta}\delta B_x. \tag{16}$$

III. SOLUTIONS FOR ALFVÉN WAVE FREQUENCY: THE PRESENCE OF A FORBIDDEN ZONE

In this section, we solve systematically the dispersion equation and eigen-relations in Eqs. (14)–(16) for Alfvén waves. The eigen-frequency of Alfvén wave depends on the values of α and β. The solutions for $\beta \gg 1$ has been previously obtained and discussed.[2,3,26,28,36–40] Here we obtain solutions of Eq. (14) for all values of α and β.

The wave frequency can be written as $\omega = \omega_r + i\omega_i$, where $\omega_r(\omega_i)$ is the real (imaginary) part of wave frequency. In order to examine the solutions, we set

$$\omega = i\xi. \tag{17}$$

Equation (15) becomes

$$\xi^3 + (1+\alpha)\beta\xi^2 + \xi + \beta = 0. \tag{18}$$

The nature of solutions in Eq. (19) is determined by the discriminant

$$\Delta = -4 - 27\beta^2 + 18(1+\alpha)\beta^2 + (1+\alpha)^2\beta^2 - 4(1+\alpha)^3\beta^4. \tag{19}$$

For $\Delta > 0$, Eq. (18) has three distinct real roots for ξ, corresponding to three purely imaginary roots for ω. Figure 2 shows that the discriminant $\Delta > 0$ in Region 2 of $\alpha - \beta$ plane with yellow color. In this region, Alfvén waves cannot propagate and become evanescent. For $\Delta = 0$, corresponding

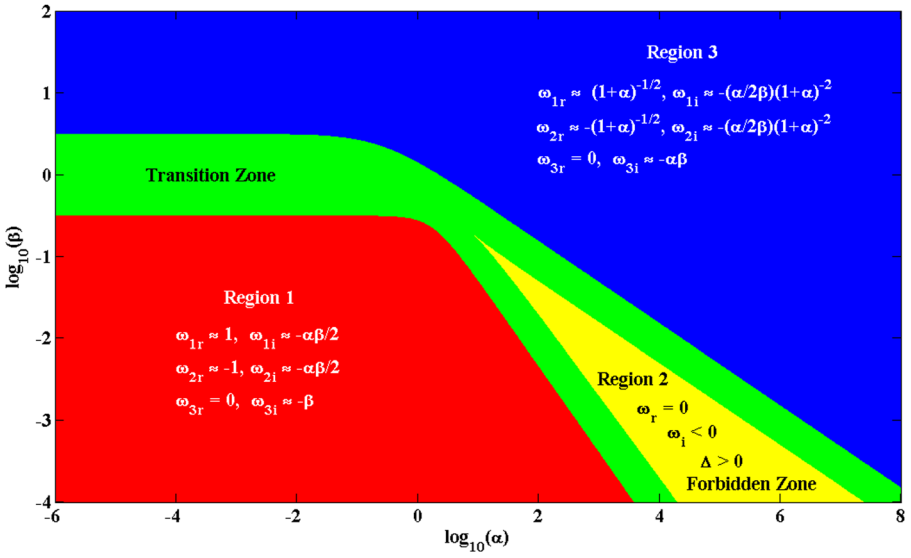

FIG. 2. The solutions of Alfvén waves can be classified into four regions in the $\alpha - \beta$ plane, where $\alpha = n_n/n_i$ is the ratio of ion and neutral density and $\beta = \nu_{ni}/\omega_0$ is the normalized collisional frequency for neutral particles by ions. In Region 1 (red) and Region 3 (blue), there are two Alfvén modes (ω_1 and ω_2) propagating in opposite direction and are purely damping mode with zero real frequency ($\omega_{3r} = 0$). In the "forbidden zone (FZ)" (Region 2, yellow), the real frequency of all three modes is zero. The green area is the transition zone between different regions.

to the boundary of Region 2, there is a multiple root and all roots are real. The tip of the forbidden zone in Region 2 is located at $(\alpha,\beta) = (8, 3^{-1.5})$.

In the area outside Region 2, which includes Region 1, Region 3, and transition region to be discussed, we have $\Delta < 0$. There is a real root and two complex conjugate roots for ξ. In this case, ω in Eq. (14) has a purely imaginary root and another two roots, which have the same imaginary part but have the same real frequency with opposite signs. The last two roots correspond to Alfvén waves propagating in opposite direction with the same damping rate.

The real and imaginary parts of Eq. (14) can be written as

$$\omega_r[{\omega_r}^2 - 3\omega_i^2 - 2(1+\alpha)\beta\omega_i - 1] = 0, \tag{20}$$

$$3{\omega_r}^2\omega_i - \omega_i^3 + (1+\alpha)\beta{\omega_r}^2 - (1+\alpha)\beta\omega_i^2 - \omega_i - \beta = 0. \tag{21}$$

(a) **Pure damping mode** ($\omega = \omega_3$) Equation (20) shows that there always is a wave mode with zero real frequency $\omega_{3r} = 0$. The corresponding imaginary part in Eq. (21) is written as

$$\omega_{3i}^3 + (1+\alpha)\beta\omega_{3i}^2 + \omega_{3i} + \beta = 0. \tag{22}$$

The value of ω_{3i} can be obtained in several limiting cases:

(a1) $\beta \ll 1$ and $\alpha\beta^2 \ll 1$ (Region 1) :

$$\omega_{3r} = 0, \omega_{3i} \approx -\beta, \tag{23a}$$

(a2) $\beta \ll 1$ and $\alpha\beta \gg 1$:

$$\omega_{3r} = 0, \omega_{3i} \approx -\alpha\beta, \tag{23b}$$

(a3) $\beta \gg 1$ and $\alpha \ll 1$:

$$\omega_{3r} = 0, \omega_{3i} \approx -\beta, \tag{23c}$$

(a4) $\beta \gg 1$ and $\alpha \gg 1$:

$$\omega_{3r} = 0, \omega_{3i} \approx -\alpha\beta. \tag{23d}$$

(b) **Propagating Alfvén modes** ($\omega = \omega_1$ and ω_2)The second factor in Eq. (20) gives

$$\omega_r^2 = 3\omega_i^2 + 2(1+\alpha)\beta\omega_i + 1. \tag{24}$$

Substituting ω_r^2 in Eq. (24) into Eq. (21), we obtain

$$8\omega_i^3 + 8(1+\alpha)\beta\omega_i^2 + 2(1+\alpha)^2\beta^2\omega_i + 2\omega_i + \alpha\beta = 0. \tag{25}$$

From Eqs. (24) and (25), we obtain the eigen-frequencies for modes 1 and 2 in several limiting cases:

(b1) $\beta \ll 1$ and $\alpha\beta \ll 1$ (Region 1) :

$$\omega_{1r} \approx 1, \quad \omega_{2r} \approx -1, \quad \omega_{1i} = \omega_{2i} \approx -\alpha\beta/2, \tag{26a}$$

(b2) $\beta \ll 1$ and $\alpha\beta^2 \gg 1$:

$$\omega_{1r} = -\omega_{2r} \approx (1+\alpha)^{-1/2}, \ \omega_{1i} = \omega_{2i} \approx -(\alpha/2\beta)(1+\alpha)^{-2}, \tag{26b}$$

(b3) $\beta \gg 1$:

$$\omega_{1r} = -\omega_{2r} \approx (1+\alpha)^{-1/2}, \ \omega_{1i} = \omega_{2i} \approx -(\alpha/2\beta)(1+\alpha)^{-2}. \tag{26c}$$

The solutions in (b3) for the case with $\beta \gg 1$ had been obtained in earlier studies.[2,3,26,28,36–40] We find here that the same solutions can also be applied to the region with $\beta \ll 1$ but $\alpha\beta^2 \gg 1$, corresponding to the right-lower part of Region 3 (blue color) in Fig. 2.

The real and imaginary parts of wave frequency for the three eigen-modes as a function of α for $\beta = 0.001$, 0.1, 10, and 1000 are plotted in Figures 3–6.

The case with $\beta = 0.001$ is shown in Fig. 3. For $\alpha \le 300$, we have $\omega_{1r} = -\omega_{2r} \approx 1$, $\omega_{3r} = 0$, $\omega_{1i} = -\omega_{2i} \approx -\alpha\beta/2$, and $\omega_{3i} = -\beta$. The real frequency $\omega_{1r}(= -\omega_{2r})$ decreases sharply to zero from $\alpha \approx 300$ to $\alpha \approx 2240$. The forbidden zone (yellow region) is located in the Region 2 with $1998 < \alpha < 250\,001$, in which all three real frequencies are zero. The damping rates are relatively large.

For $\alpha > 10^6$, the real frequency can be expressed as $\omega_{1r} = -\omega_{2r} \approx (1+\alpha)^{-1/2}$ and the imaginary part $\omega_{1i} = \omega_{2i} \approx -(\alpha/2\beta)(1+\alpha)^{-2}$. For the damping mode with $\alpha > 10^6$, we have $\omega_{3r} = 0$ and $\omega_{3i} = -\alpha\beta$.

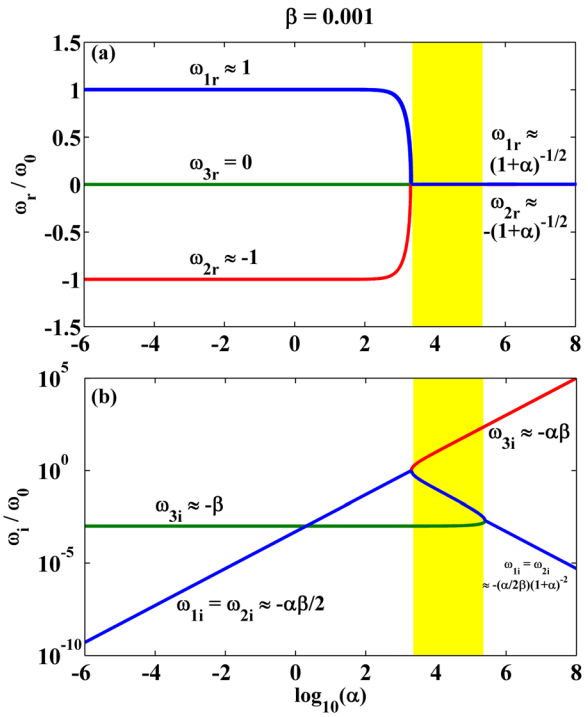

FIG. 3. The real part (ω_r) and imaginary part (ω_i) of the wave frequency of three eigen-modes are plotted as a function of the density ratio $\alpha = n_n/n_i$ for $\beta = \nu_{ni}/\omega_0 = 0.001$. The real frequency $\omega_{1r}(\omega_{2r})$ is shown by the blue (red) line in the top figure. The damping rates $|\omega_{1i}|$ and $|\omega_{2i}|$ have the same value and are shown by the same blue line in the bottom figure. The yellow area is FZ with $\omega_{1r} = \omega_{2r} = \omega_{3r} = 0$. As the value of α approaches the yellow zone from the left, the real frequency of ω_{1r} and $|\omega_{2r}|$ decreases sharply to zero. On the right hand side of the yellow region, the real frequency of modes 1 and 2 can be expressed as $\omega_{1r} = -\omega_{2r} \approx (1+\alpha)^{-1/2}$.

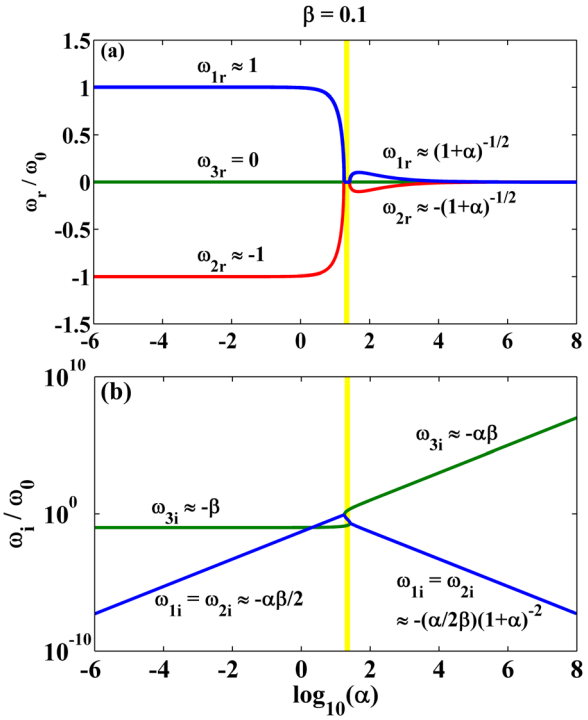

FIG. 4. Same as Fig. 3 except that FZ (yellow) is very narrow.

Fig. 4 shows the real and imaginary frequencies for $\beta = 0.1$. The results are similar to the case for $\beta = 0.001$ except that the range for forbidden zone is small ($17.87 < \alpha < 26.04$).

Cases with $\beta = 10$ and 1000 are shown in Figs. 5 and 6. The real frequencies are $\omega_{1r} = -\omega_{2r} \approx (1+\alpha)^{-1/2}$ and $\omega_{3r} = 0$. The imaginary part $\omega_{1i} = \omega_{2i} \approx -(\alpha/2\beta)(1+\alpha)^{-2}$ for the whole range of α. For the pure damping mode, $\omega_{3i} = -\beta$ for $\alpha \ll 1$ and $\omega_{3i} \approx -\alpha\beta$ for $\alpha \gg 1$.

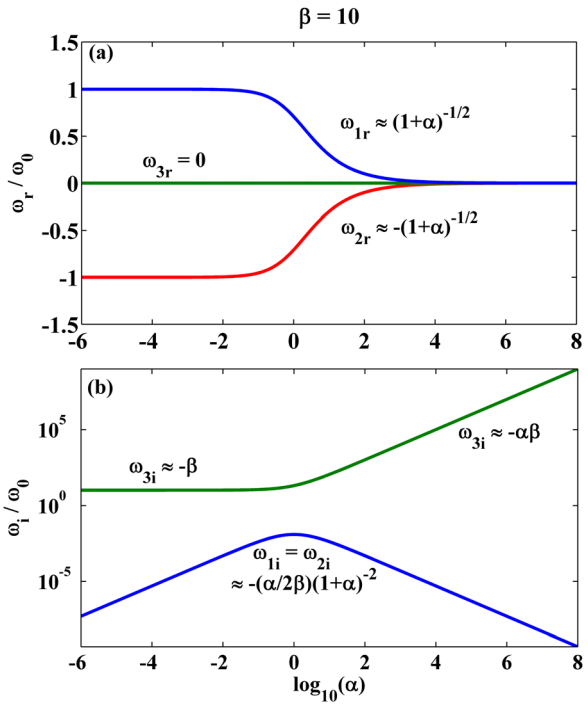

FIG. 5. The real (ω_r) and imaginary (ω_i) part of wave frequency for three eigen-modes are plotted as a function of $\alpha = n_n/n_i$ for $\beta = \nu_{ni}/\omega_0 = 10$.

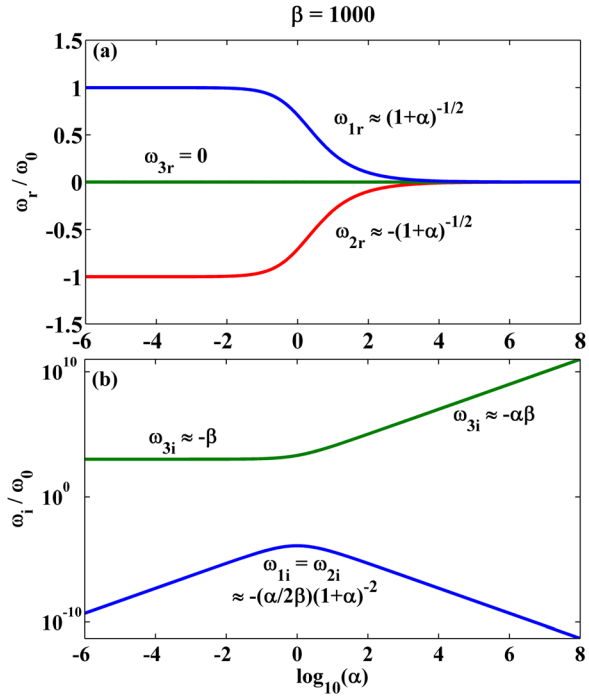

FIG. 6. Same as Fig. 3.

In Figure 7, we plot the eigen-amplitude and phase angle ϕ relative to δB_x of two propagating Alfvén modes with ω_1 and ω_2 as a function of α for $\beta = 0.001$ (left panel) and $\beta = 1000$ (right panel). From Eqs. (15) and (16), we have amplitude ratio $|\delta v_{ix}/\delta B_x| = |\omega|$ and $|\delta v_{nx}/\delta B_x| = |\omega\beta/(i\omega - \beta)|$. For $\beta = 0.001$, the amplitude $|\delta v_{1ix}/\delta B_x| = |\delta v_{2ix}/\delta B_x| \approx 1$ and $|\delta v_{1nx}/\delta B_x| = |\delta v_{2nx}/\delta B_x| \approx \beta$ on the left side of yellow zone. The velocity δv_{1ix} is out of phase with δB_x (relative phase angle $\phi = 180°$) while δv_{2ix} is in phase with δB_x ($\phi = 0°$). The phase angle for the neutral velocities δv_{1nx} and δv_{2nx} is $\phi = -90°$. This means that when the ion-neutral collision frequency is much lower than the wave frequency, the oscillation of ions and neutrals is 90° out of phase with each other, and the oscillation amplitude of ions is much greater than that of neutrals.

For $\beta = 1000$, the amplitude $|\delta v_{1ix}/\delta B_x| = |\delta v_{2ix}/\delta B_x| = |\delta v_{1nx}/\delta B_x| = |\delta v_{2nx}/\delta B_x| = (1+\alpha)^{-1/2}$. The phase angle of δv_{1ix} and δv_{1nx} is $\phi = 180°$ while the phase angle of δv_{2ix} and δv_{2nx} is $\phi = 0°$ relative to δB_x. In this case, ions and neutrals oscillate synchronously as a whole with the same amplitude and same phase. The above eigen-mode characteristics are valid for cases with $\beta \gg 1$.

IV. SOLUTION FOR ALFVÉN WAVENUMBER: THE PRESENCE OF HEAVY DAMPING ZONE

In the last section, we have obtained the solution for real and imaginary frequencies, ω_r and ω_i, for a given wavenumber k, in the $\alpha - \beta$ space. However, in a physical situation the Alfvén wave is excited at some frequency and propagates along the magnetic field line or at angle oblique to magnetic field line. The wavenumber k will adjust itself to obey the dispersion equation (13). In this section, we obtain the wavenumber k from the dispersion equation (13) for Alfvén wave with a fixed frequency $\omega = \omega_0$.

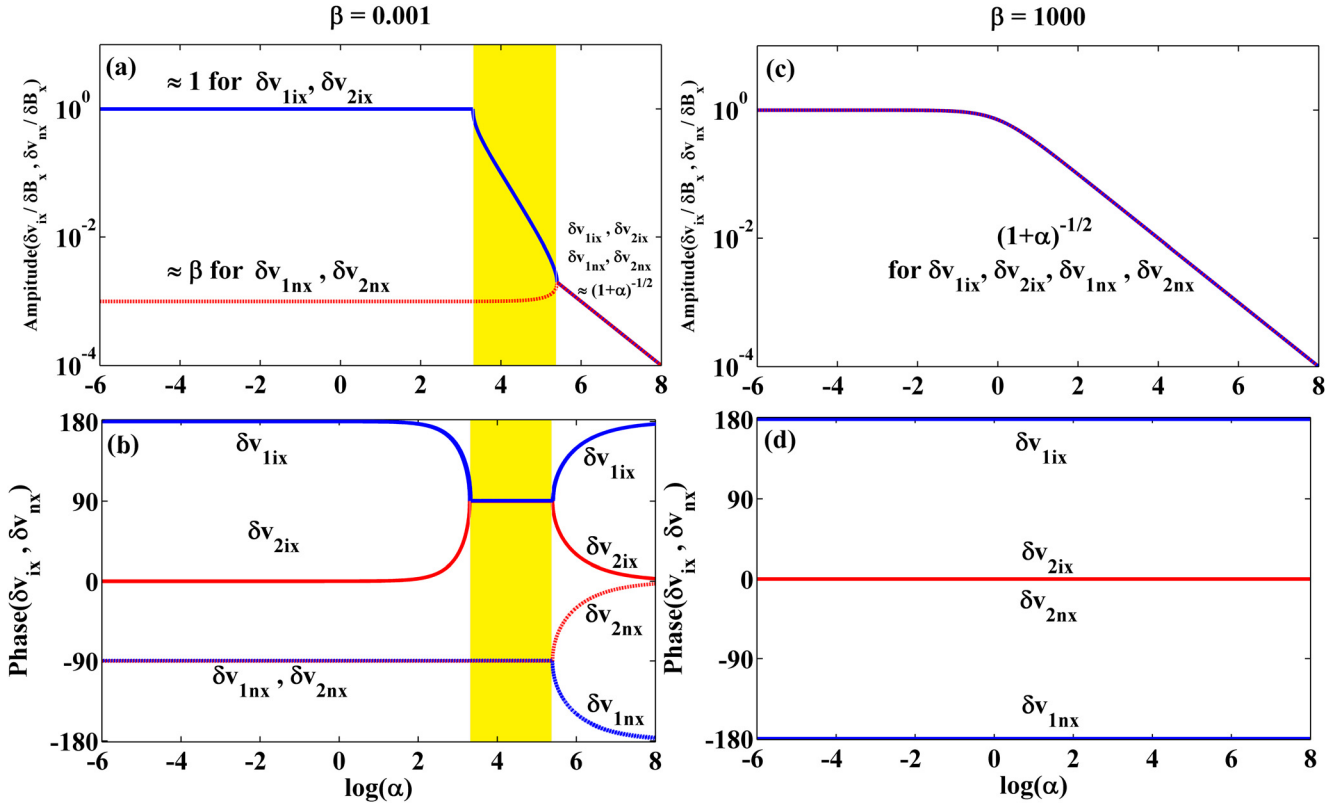

FIG. 7. The eigen-amplitudes, $\delta v_{ix}/\delta B_x$ and $\delta v_{nx}/\delta B_x$, and phases of two propagating Alfvén modes with ω_1 and ω_2 as a function of $\alpha = n_n/n_i$ for $\beta = \nu_{ni}/\omega_0 = 0.001$ (left) and $\beta = 1000$ (right). For $\beta = 0.001$, $|\delta v_{1ix}/\delta B_x| = |\delta v_{2ix}/\delta B_x| \approx 1$ and $|\delta v_{1nx}/\delta B_x| = |\delta v_{2nx}/\delta B_x| \approx \beta$ on the left side of forbidden zone, while $|\delta v_{1i}/\delta B_x| = |\delta v_{2i}/\delta B_x| = |\delta v_{1n}/\delta B_x| = |\delta v_{2n}/\delta B_x| \approx (1+\alpha)^{-1/2}$. For $\beta = 1000$, $\delta v_{1ix}/\delta B_x = \delta v_{2ix}/\delta B_x = \delta v_{1nx}/\delta B_x = \delta v_{2nx}/\delta B_x \approx (1+\alpha)^{-1/2}$ and the ion and neutral velocity of mode 1 (mode 2) are out of phase (in phase) with δB_x.

We define $k_0 = \omega_0/V_A\cos\theta$, $\beta = \nu_{ni}/\omega_0$, and $\alpha = n_n/n_i$ as before. Eq. (13) leads to the following equation for k^2:

$$\left(\frac{k}{k_0}\right)^2 = \frac{1+i\beta(1+\alpha)}{1+i\beta}. \tag{27}$$

Write k = $k_r + ik_i$. In Figure 8, $|k_r|$ and $|k_i|$ are plotted as a function of α for $\beta = 10^{-9}$, 10^{-8}, 10^{-7},..., and 10^{6}. Fig. 8(a) indicates that k_r increases as α increases. It is noted that the k_r curve for $\beta > 10$ is nearly the same as the curve for $\beta = 10$. The solution in Eq. (27) will give two damping modes propagating in opposite direction.

The yellow sections of lines in Figs. 8(a) and 8(b) correspond to those with $\alpha - \beta$ values in FZ of Fig. 2. It is found from Fig. 8(b) that the value of $|k_i|/k_0$ reaches ~1 as each curve reaches the yellow sections (FZ) from below. The wave damping in space is given by $e^{-|k_i|z} \cong e^{-2\pi}$ for z $= \lambda$ (wavelength) $= 2\pi/k_0$ and $|k_i| \cong k_0$. It is interesting to note that $|k_i|$ keeps increasing with increasing α after the curve goes beyond the yellow FZ. It is thus expected that as Alfvén waves propagate into FZ, the waves will be heavily damped. On the other hand, $|k_i|$ decreases with increasing β for a given value of α as shown in Fig. 8(c).

In Fig. 9, the contours of $|k_r/k_0|$ and $|k_i/k_0|$ are plotted in the $\alpha - \beta$ plane, similar to that shown in Fig. 2. The contour line with $|k_i/k_0| = 1$ is plotted in Fig. 9(b). The lower section of the contour line is very close to the left boundary of FZ in Fig. 2. Alfvén waves are expected to be heavily damped in the region on the right-hand side of the contour line. The region with $|k_i/k_0| \geq 1$ will be called the "heavy damping zone (HDZ)."

We use Eqs. (8)–(10) to simulate the damping of Alfvén wave as the wave propagates into a region with $\alpha - \beta$ values in FZ. Fig. 10(d) plots the spatial profile of α, which is set to $\alpha = \alpha_1 = 0.1$ for z < 30 and increases to $\alpha = \alpha_2 = 10^4$ for z > 40. In the simulation, we set $\beta = 0.001$. In Fig. 10(d), the yellow region corresponds to the range of α in FZ of Fig. 2 for $\beta = 0.001$. We use the eigenvector in Eq. (12) to excite wave with a fixed frequency at z = 0. Figs. 9(a)–9(c) show the spatial profiles of δB_x, δV_{ix}, and δV_{nx} at a time after the wave propagates out of the simulation boundary. The wave is heavily damped as the wave reaches FZ at z ≅ 40.

In order to see the damping rate, we plot in Figs. 10(e)–10(h) the spatial profiles of $|\delta B_x{}^2|$ in log scale for $\alpha_2 = 10^4, 10^3, 10^2$, and 10^1. For $\alpha_2 = 10^4$, $|\delta B_x{}^2|$ decreases by a factor of $10^{-7.5}$ within a distance of $k_0\Delta z \cong 4$. This corresponds to $|k_i/k_0| \cong 2.2$ and is consistent with the theoretical value shown in Fig. 8(b). From the slop of blue lines in Figs. 10(f) and 10(g), we obtain $|k_i/k_0| \cong 0.46$ for $\alpha_2 = 10^3$ and $|k_i/k_0| = 0.05$ for $\alpha_2 = 10^2$, consistent with the values in Fig. 8(b). For $\alpha_2 = 10$, the wave damping is very weak.

V. APPLICATION TO ALFVÉN WAVES IN THE IONOSPHERE AND SOLAR CHROMOSPHERE

In this section, we consider low frequency transverse Alfvén waves in the ionosphere and solar chromosphere. In

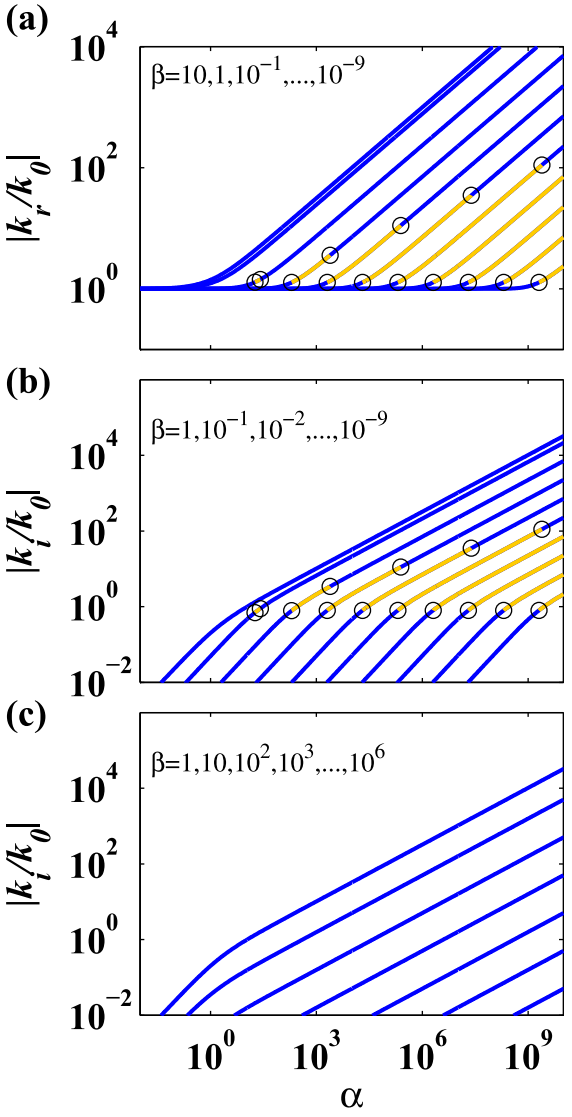

FIG. 8. The real and imaginary parts of the wavenumbers, $|k_r/k_0|$ and $|k_i/k_0|$, are plotted as a function of α for $\beta = 10^{-9}, 10^{-8}, \ldots,$ and 10^6. The curve of $|k_r/k_0|$ for $\beta > 10$ is nearly the same as the curve for $\beta = 10$ in (a). The yellow sections of lines in (a) and (b) correspond to those with $\alpha - \beta$ values in FZ of Fig. 2.

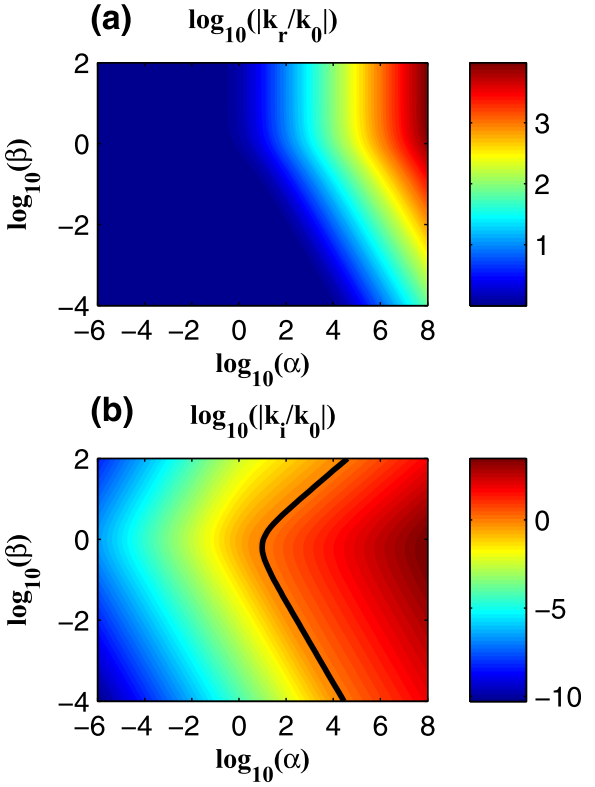

FIG. 9. The contours of (a) $|k_r/k_0|$ and (b) $|k_i/k_0|$ are plotted in the $\alpha - \beta$ plane. The contour with $|k_i/k_0| = 1$ is shown by the black line. The region with $|k_i/k_0| \geq 1$ is termed "the heavy damping zone (HDZ)."

the ionosphere and chromosphere, the damping effects of dense neutral particles on Alfvén waves are very important. In particular, we want to identify the presence of FZ and HDZ in the ionosphere and solar chromosphere for some range of Alfvén frequency $\omega_0 = kV_A\cos\theta$.

Fig. 11(a) shows the vertical density profiles of ions (n_i) and neutrals (n_n) in daytime and nighttime ionosphere during solar quiet time. The ion and neutral densities are calculated using empirical MESIS and IRI models. We consider the height profiles of daytime and nighttime ionosphere at low–altitude (20 °N) in the equinox of 2008. The corresponding density ratio, $\alpha = n_n/n_i$, is plotted in Fig. 11(c). Below 700 km, the value of α in the nighttime ionosphere is greater than that in daytime ionosphere. Based on the empirical foumula listed in Richmond,[42] the collisional frequency ν_{ni} of neutral particles from a collision with ions are calculated as shown in Fig. 11(b). In daytime ionosphere, the higher value of ion density causes higher collisional frequency ν_{ni}. Hence, collisional frequency ν_{ni} has one order of magnitude greater than that for nighttime ionosphere. Two cases with Alfvén frequency ($\omega_0 = 10^{-2}$ and 10^{-4}s^{-1}) are considered. We plot the corresponding $\beta = \nu_{in}/\omega_0$ for the daytime and nighttime ionosphere in solid lines and dashed lines in Figs. 11(d) and 11(f).

Based on FZ plotted in the $\alpha - \beta$ plane of Fig. 2, HDZ of Fig. 9, and the vertical profiles of α in Fig. 11(c), we draw FZ (enclosed by red solid line) and HDZ (enclosed by blue dot line) for the daytime (Fig. 11(d)) and nighttime (Fig. 11(f)) ionosphere. In FZ, the real frequency of Alfvén wave becomes zero. In both FZ and HDZ, waves are heavily damped. Fig. 11(d) shows that the curve for Alfvén frequency $\omega_0 = 10^{-4}\text{s}^{-1}$does not pass through FZ but pass through HDZ. Alfvén wave with frequency $\omega_0 = 10^{-2}\text{s}^{-1}$ passes through both FZ and HDZ in the ionosphere. It can also be found from Figs. 11(d) and 11(f) that for Alfvén wave with frequency $\omega_0 > 10^{-2.6}\text{s}^{-1} \approx 2.5 \times 10^{-3}\text{s}^{-1}$ $(f_0 \approx 0.4\,\text{mHz})$ will pass through the daytime FZ, and the curve with $\omega_0 > 10^{-3.7}\text{s}^{-1} \approx 2.0 \times 10^{-4}\text{s}^{-1} (f_0 \approx 0.03\,\text{mHz})$ will encounter the nighttime FZ. The HDZ in Figs. 11(d) or 11(f) shows that Alfvén waves with $1\,\text{Hz} > f_0 > 10^{-5}\text{Hz}$ are expected to be highly damped in the ionosphere.

Alfvén waves in the solar chromosphere can be generated by the magnetic-field fluctuations or driven by the plasma convection motion in the supergranulation. Alfvén waves are low-frequency transverse waves with frequency lower than proton cyclotron frequency. The strength of

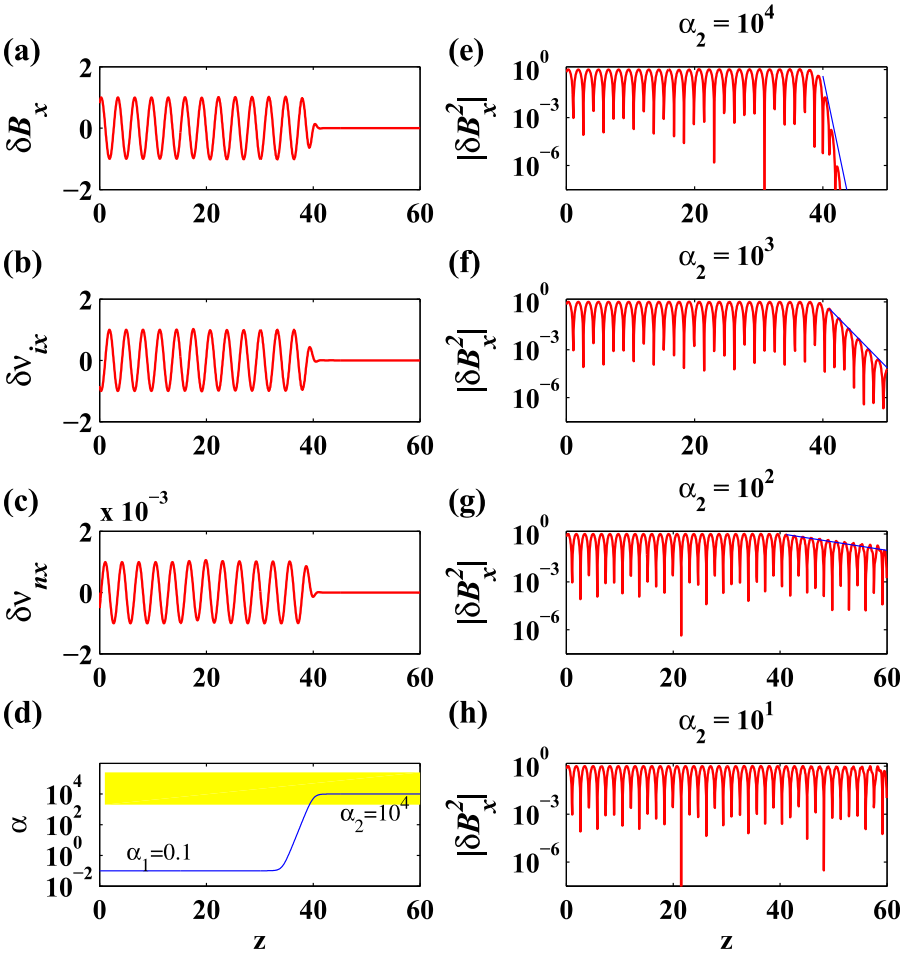

FIG. 10. (a)–(c) The spatial profiles of δB_x, δV_{ix}, and δV_{nx} of Alfvén wave injected from the left boundary ($z = 0$) with $\beta = 0.001$ and the spatial profile of α in (d). The yellow region corresponds to FZ for $\beta = 0.001$. (e)–(h) The spatial profiles of $|\delta B_x{}^2|$ for four simulation cares with $\alpha_2 = 10^4$, 10^3, 10^2, and 10.

magnetic field in the solar chromosphere is ≈10 G and proton cyclotron frequency $\Omega_p \approx 10^5 s^{-1}$.

Fig. 12(a) shows the neutral (n_n) and ion (n_i) density profiles in the solar chromosphere. The neutral and ion densities are obtained from the results of VAL C model.[43] The collisional frequency (ν_{ni}) for a neutral particle by ions is adopted from the earlier work.[28] The corresponding profiles of $\alpha = n_n/n_i$ and $\beta = \nu_{ni}/\omega_0$ for $\omega_0 = 10^{-4}$, 1 and $10^4 s^{-1}$ are plotted in Figs. 12(c) and 12(d). The corresponding FZ of Alfvén waves is enclosed by the red solid line while the HDZ is enclosed by the blue dashed line. As shown in Fig. 12(d), the curve with Alfvén frequency $\omega_0 = 10^4\, s^{-1}$ encounters FZ and HDZ. Note that Alfvén frequency $\omega_0 = 10^4 s^{-1}$ is only one order lower than proton cyclotron frequency $\approx 10^5 s^{-1}$. Fig. 9(d) shows that the curve with Alfvén frequency $\omega_0 \geq 10^{3.4} s^{-1} \approx 2.5 \times 10^3 s^{-1}$ ($f_0 \approx 400$ Hz) will encounter FZ, and waves with $\omega_0 \geq 1 s^{-1}$ will encounter HDZ in the partially ionized chromosphere.

VI. SUMMARY

In summary, we have systematically solved the Alfvén dispersion equation and obtained the eigen-modes to examine the effects of ion-neutral collisions. We also apply our results to partially ionized plasmas in earth's ionosphere and solar chromosphere. The main results are listed below.

(1) The eigen-frequency and damping rate of Alfvén waves depend on two parameters: $\alpha = n_n/n_i$ and $\beta = \nu_{ni}/\omega_0$. There exists a "forbidden zone (FZ)" as well as a "heavy damping zone (HDZ)" in the $\alpha - \beta$ parameter plane. The real frequency of Alfvén waves is zero in FZ for waves with a fixed wavenumber k. For waves with a fixed frequency ω, the imaginary part of wave number $|k_i| \geq k_0 = \omega/V_A \cos\theta$ in HDZ. Alfvén waves are heavily damped as the waves propagate into FZ or HDZ.
(2) Outside FZ, there are three eigen-modes: one purely damping mode (ω_3) and two Alfvén wave modes (ω_1 and ω_2) propagating in opposite direction with the same damping rate.
(3) In the case with $\beta = \nu_{ni}/\omega_0 \gg 1$, two propagating Alfvén modes have real frequency $\omega_{1r} = -\omega_{2r} \approx (1+\alpha)^{-1/2}\omega_0$ and damping rate $\omega_{1i} = \omega_{2i} \approx -(\alpha/2\beta)(1+\alpha)^{-2}\omega_0$, where $\omega_0 = kV_A \cos\theta$.
(4) In the case with $\beta \ll 1$ and $\alpha\beta^2 \ll 1$ (Region 1), we have $\omega_{1r} = -\omega_{2r} \approx \omega_0$ and $\omega_{1i} = -\omega_{2i} \approx -(\alpha\beta/2)\omega_0$.
(5) In the case with $\beta \ll 1$ and $\alpha\beta^2 \gg 1$, we have $\omega_{1r} = -\omega_{2r} \approx (1+\alpha)^{-1/2}\omega_0$ and $\omega_{1i} = \omega_{2i} \approx -(\alpha/2\beta)(1+\alpha)^{-2}\omega_0$.
(6) In the ionosphere, Alfvén waves with frequency $f_0 > 0.4$ mHz ($f_0 > 0.03$ mHz) will encounter the daytime (nighttime) FZ. Alfvén waves with $1\text{Hz} > f_0 > 10^{-5}$Hz will pass through HDZ and be heavily damped.
(7) In the solar chromosphere Alfvén waves with frequency $f_0 < 400$ Hz will not encounter FZ while Alfvén waves with $f_0 > 2$ Hz will encounter HDZ.

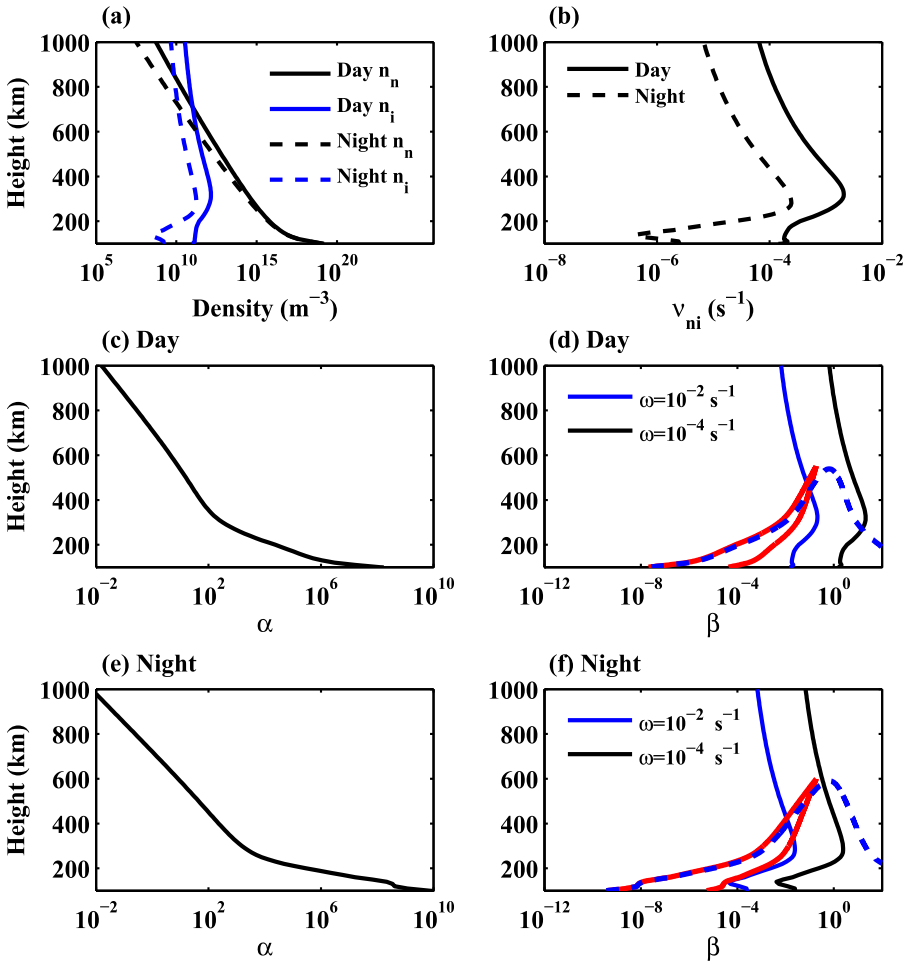

FIG. 11. The vertical profiles of (a) neutral (n_n) and ion density (n_i) for daytime and nighttime ionosphere, indicated by solid and dashed lines, (b) the collision frequency (ν_{ni}) for a neutral particle to collide with ions in the daytime and nighttime ionosphere, (c), (e) the ratio of neutral density to ions density($\alpha = n_n/n_i$), and (d), (f) the parameter $\beta = \nu_{ni}/\omega_0$ for the daytime and nighttime ionosphere in blue line and black line for $\omega_0 = 10^{-2}$ and $10^{-4}s^{-1}$. The FZ (HDZ) for shear Alfvén waves is enclosed by red solid (blue dashed) line.

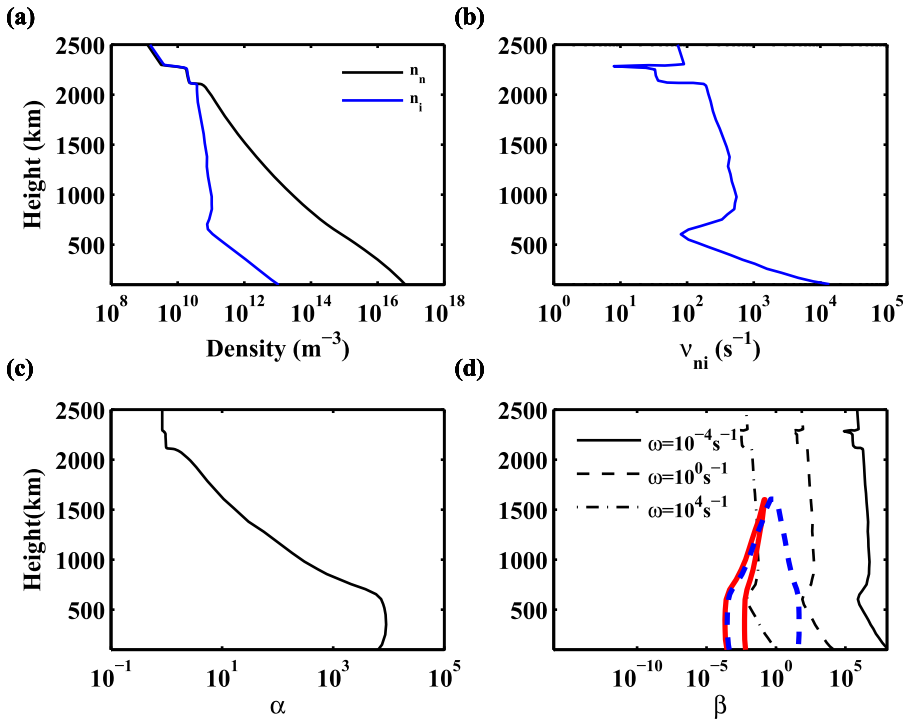

FIG. 12. (a) The neutral and ion density profiles in the solar chromosphere, indicated by black and blue lines; (b) the vertical profile of collisional frequency (ν_{ni}) for a neutral particle to collide with ions in the solar chromosphere; (c) profile of the ratio of neutral density to ion density, $\alpha = n_n/n_i$; and (d) profile of $\beta = \nu_{ni}/\omega_0$ for $\omega_0 = 10^{-4}$, 10^0, and $10^4 s^{-1}$ (solid, dashed, and point-dashed lines). The FZ (HDZ) of Alfvén waves is enclosed by red solid (blue dashed) line.

ACKNOWLEDGMENTS

This work was partially supported by a grant from National Cheng Kung University, grants from the National Science Council to Academia Sinica (NSC 101-2628-M-001-007-MY3) and to the National Central University (NSC 99-2111-M-008-017-MY3 and NSC 102-2111-M-008-001), and by the Chinese Academy of Sciences under Grant Nos. KZCX2-YW-QN512 and KZCX2-YW-N28.

[1]H. Alfvén, Nature (London) **150**, 405 (1942).
[2]J. H. Piddington, MNRAS **116**, 314 (1956).
[3]R. Kulsrud and W. P. Pearce, Astrophys. J. **156**, 445 (1969).
[4]J. W. Belcher and L. Davis, Jr., J. Geophys. Res. **76**, 3534, doi:10.1029/JA076i016p03534 (1971).
[5]T. H. Stix, *Waves in Plasmas* (American Institute of Physics, New York, 1992).
[6]J. V. Hollweg and P. A. Isenberg, J. Geophys. Res. **107**, 1147, doi:10.1029/2001JA000270 (2002).
[7]P. Song, V. M. Vasyliūnas, and L. Ma, J. Geophys. Res. **110**, A09309, doi:10.1029/2005JA011139 (2005).
[8]S. R. Cranmer, A. A. van Ballegooijen, and R. J. Edgar, Astrophys. J. Suppl. **171**, 520 (2007).
[9]S. R. Cranmer, Living Rev. Sol. Phys. **6**, 3 (2009).
[10]J. V. Hollweg, J. Astrophys. Astron. **29**, 217 (2008).
[11]P. Song, V. M. Vasyliūnas, and X. Z. Zhou, J. Geophys. Res. **114**, A08213, doi:10.1029/2008JA013629 (2009).
[12]P. Song and V. M. Vasyliūnas, J. Geophys. Res. **116**, A09104, doi:10.1029/2011JA016679 (2011).
[13]P. A. Isenberg, M. A. Lee, and J. V. Hollweg, J. Geophys. Res. **106**, 5649, doi:10.1029/2000JA000099 (2001).
[14]L. Chen, Z. Lin, and R. B. White, Phys. Plasmas **8**, 4713 (2001).
[15]B. Wang, C. B. Wang, P. H. Yoon, and C. S. Wu, Geophys. Res. Lett. **38**, L10103 (2011).
[16]J. R. Jokipii, Astrophys. J. **156**, 1107 (1969).
[17]A. Hasegawa and L. Chen, Phys. Rev. Lett. **36**, 1362 (1976).
[18]H. Alfvén, *On the Origin of the Solar System* (Clarendon, Oxford, 1954).
[19]J. H. Piddington, MNRAS **114**, 638 (1954).
[20]J. H. Piddington, MNRAS **114**, 651 (1954).
[21]B. Lehnert, Nuovo Cimento, Suppl. **13**, 59 (1959).
[22]D. E. Osterbrock, Astrophys. J. **134**, 347 (1961).
[23]L. Hartmann and K. B. MacGregor, Astrophys. J. **242**, 260 (1980).
[24]E. G. Zweibel, Astrophys. J. **340**, 550 (1989).
[25]J. D. Huba, "Universal interchange instability in partially ionized gases," Phys. Fluids B **2**, 2547 (1990).
[26]G. Haerendel, Nature (London) **360**, 241 (1992).
[27]B. De Pontieu and G. Haerendel, Astron. Astrophys. **338**, 729 (1998).
[28]B. De Pontieu, P. C. H. Martens, and H. S. Hudson, Astrophys. J. **558**, 859 (2001).
[29]S. P. James and R. Erdélyi, Astron. Astrophys. **393**, L11 (2002).
[30]S. P. James, R. Erdélyi, and B. De Pontieu, Astron. Astrophys. **406**, 715 (2003).
[31]R. Erdélyi and S. P. James, Astron. Astrophys. **427**, 1055 (2004).
[32]B. Roberts, Sol. Phys. **69**, 27 (1981).
[33]B. Roberts, *In Advances in Solar System Magnetohydrodynamics* (Cambridge University Press, 1991).
[34]C. Uberoi and A. Datta, Phys. Plasmas **5**, 4149 (1998).
[35]R. L. Lysak, J. Geophys. Res. **104**, 10017, doi:10.1029/1999JA900024 (1999).
[36]N. Kumar and B. Roberts, Sol. Phys. **214**, 241 (2003).
[37]R. M. Evans, M. Opher, V. Jatenco-Pereira, and T. I. Gombosi, Astrophys. J. **703**, 179 (2009).
[38]T. V. Zaqarashvili, M. L. Khodachenko, and H. O. Rucker, Astron. Astrophys. **534**, A93 (2011).
[39]T. C. Mouschovias, G. E. Ciolek, and S. A. Morton, MNRAS **415**, 1751 (2011).
[40]A. A. Mamun and P. K. Shukla, Astrophys. J. **548**, 269 (2001).
[41]B. H. Wu, J. M. Wang, and L. C. Lee, Geophys. Res. Lett. **28**, 3051, doi:10.1029/2001GL012958 (2001).
[42]D. Richmond, *Handbook of Atmospheric Electrodynamics* (CRC, Boca Raton, FL, 1995), Vol. 2, p. 249.
[43]J. E. Vernazza, E. H. Avrett, and R. Loeser, Astrophys. J. Suppl. Ser. **45**, 635 (1981).